Pergamon

Int. J. Heat Mass Transfer. Vol. 39, No. 17, pp. 3649–3657, 1996

0017–9310/96 $15.00 + 0.00

PII: S0017–9310(96)00034–8

Comparison of some inverse heat conduction methods using experimental data

J. V. BECK

Heat Transfer Group, Department of Mechanical Engineering, Michigan State University, East Lansing, MI 48824-1226, U.S.A.

B. BLACKWELL

Sandia National Laboratories, Albuquerque, NM 87185, U.S.A.

and

A. HAJI-SHEIKH

Department of Mechanical Engineering, University of Texas at Arlington, Arlington, TX 76019-0023, U.S.A.

(*Received* 27 *March* 1995 *and in final form* 19 *January* 1996)

Abstract—This paper compares several methods of finding the surface heat flux using transient temperature measurements inside a heat-conducting body. Experimental data is used with a known heat flux history. The methods include function specification with several future approximations, Tikhonov regularization, iterative regularization and specified functions over large time regions with Green's functions. The first three methods are used with the residual principle and the results are quite similar. If the heat flux has a simple time variation over large time regions, taking advantage of that feature can improve the results, as shown by the Green's function analysis. Copyright © 1996 Elsevier Science Ltd.

INTRODUCTION

The inverse heat conduction problem (IHCP) is the determination of the surface heat flux history from interior transient temperature measurements in a solid. Although many papers and books have been written on the IHCP, few provide both experimental heat flux values and a comparison of several methods. This paper includes these features and a use of the residual principle.

In Alifanov [1] a history of the IHCP is given, going back even to the nineteenth century. However, the earliest engineering paper may be due to Shumakov [2] in 1957 in the Soviet Union. Better known in the United States is the paper by Stolz in 1960 [3]. The papers by Shumakov and Stolz solved the problem in a sequential manner that did not change the basic physical treatment of the problem; they did not consider the lag and damping of the measurements (particularly as the time steps become small), which result in the problem becoming ill-posed. A method that treated the lag/damping effects is due to Beck and is called the function specification method [4–10]. It has the two advantages that (a) it is simple in concept and (b) it does not change the physics of the problem, since the intrinsic parabolic nature of the problem is unchanged. The function specification method (FSM) is sequential in nature and thus is computationally efficient and, perhaps more important, the measurements in the distant future do not affect the 'present' estimates, as for other methods to be described.

Another important method that is simple in concept and has sequential aspects is the mollification method of Murio [11]. This method has a substantial mathematical basis.

Two other very important methods are Tikhonov regularization [8, 12] and iterative regularization [1, 13]. These methods are usually presented as whole domain methods in which all the heat flux components are simultaneously estimated for all times (and position, if multidimensional). Two advantages of these methods are that they have had rigorous mathematical investigation and can be applied very generally. They are clearly very important methods. The generality of the whole domain analysis comes at the expense of greater computational and programming burdens and more difficult analysis. Also, it changes the physical problem from one with causal aspects to one in which the later measurements affect even the earliest times. However, ref. [8] shows that the sequential concepts in the FSM can be incorporated in the Tikhonov regularization method. The whole domain concept can also be applied using Green's functions, provided the problem is linear.

The basic objective of this paper is to provide a realistic comparison of several methods for the solu-

NOMENCLATURE

C	volumetric heat capacity [J m^{-3} K^{-1}]	x	coordinate
G	Green's function [m^{-1}]	X	sensitivity coefficient, equation (9)
I	number of measured times	y	coordinate for Green's function analysis
J	number of sensor locations	Y	measured temperature [°C].
k	thermal conductivity [W m^{-1} K^{-1}]		
L	length of a region [m]		
N	number of measurements at time t	Greek symbols	
q	heat flux [W m^{-2}]	α	Tikhonov regularization parameter
r	number of future times for function specification	σ	root mean square for q [W m^{-2}]
		τ	dimensionless time.
s_Y	standard deviation of Y		
S	sum of squares function, equation (11) or (12)	Subscripts	
		i	time index
S_M	S for function specification method	j	space index
t	time [s]	M	time index
T	temperature [°C]	rms	root mean square.

tion of the IHCP. The same criterion (namely the residual principle) for selecting the various parameters is used for most of the methods. For the FSM, the parameter is the number of future times; for the iterative regularization method, the parameter is the number of iterations; and for Tikhonov regularization, it is the regularizing parameter. Although zeroth-, first- and second-order Tikhonov regularizations exist, this paper focuses on the zeroth-order.

A brief outline of the paper is given. First, a mathematical description of the IHCP is displayed. Next an experiment and associated measurements are shown. This is followed by a comparison of several methods, and finally conclusions.

MATHEMATICAL DESCRIPTION OF THE IHCP

The one-dimensional IHCP for three layers of different materials is mathematically described as (see Fig. 1)

$$\frac{\partial}{\partial x}\left[k_s\frac{\partial T_s}{\partial x}\right]=C_s\frac{\partial T_s}{\partial t},\ L_{s-1}<x<L_s,\quad s=1,2,3. \tag{1a}$$

The initial temperature is T_0 in each region. Measurements are given at J locations and

$$k_s\left.\frac{\partial T_s}{\partial x}\right|_{L_s^-}=k_{s+1}\left.\frac{\partial T_{s+1}}{\partial x}\right|_{L_s^+},\quad s=1,2 \tag{1b}$$

$$T_s|_{L_s^-}=T_{s+1}|_{L_s^+},\quad s=1,2 \tag{1c}$$

$$\left.\frac{\partial T}{\partial x}\right|_{L_3}=0 \tag{1d}$$

$$T_s(x,0)=T_0,\quad s=1,2,3 \tag{1e}$$

I times,

$$T(x_j,t_i)=Y_j(t_i),\quad i=1,\ldots,I;\quad j=1,\ldots,J. \tag{2}$$

The objective is to calculate the surface heat flux history (at $x=0$).

$$-k_1\left.\frac{\partial T_1}{\partial x}\right|_{x=0}=q(t)=? \tag{3}$$

EXPERIMENT

An experiment was done with two identical specimens with a mica heater between them; this approach yields symmetric boundary conditions, with equal heat fluxes toward each side at the heater center line. Figure 1 shows only one-half of the symmetric geometry. At the nonheated surfaces of the specimen, ceramic insulation was used. The plane heating element was in the center of the mica heater ($x=0$) and was very thin compared with the total thickness of the mica heater (0.86 mm). Therefore, an unknown heat flux condition was used at $x=0$ in the IHCP. Parameter techniques were used to estimate the thermal properties of each layer; see Table 1. One half of the mica thickness and the interface conductance were modeled as a single effective material. A series of short experiments (about 1 s in duration) was done to estimate the effective thermal properties of the mica-interface conductance [14, 15].

At the mica–specimen interface, seven thermocouples produced consistent readings. Rather than using seven separate values, an average of these read-

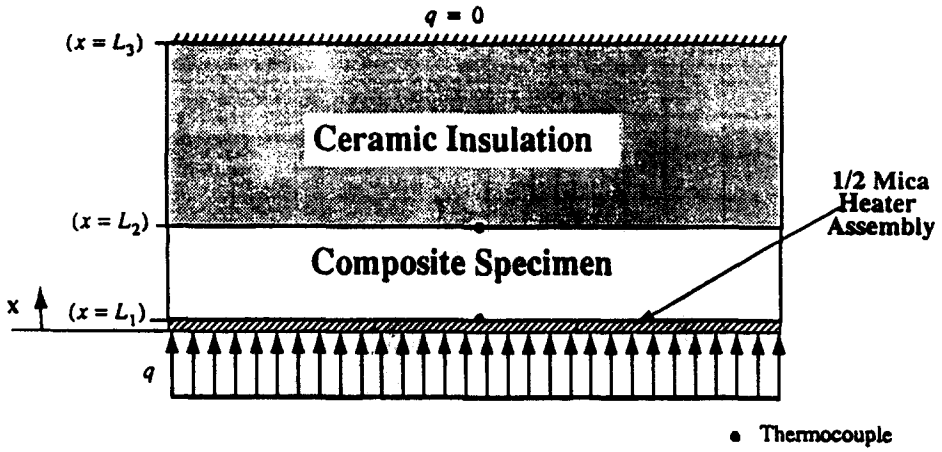

Fig. 1. Schematic of one half of the geometry of the experiment. The missing lower half is symmetric about $x = 0$.

Table 1. Thermal properties of test specimen

Material	Thermal conductivity ($W\,m^{-1}\,K^{-1}$)	Volumetric heat capacity $\times 10^{-6}$ ($J\,m^{-3}\,K^{-1}$)	Thickness (mm)
Mica heater	0.142	2.03	0.43
Carbon–carbon	3.40	1.42	9.14
Ceramic insulation	0.088	0.419	25.4

ings at each time step was used. Let the temperature at time t_i and sensor j be denoted, Y_{ij}. The average at time t_i is

$$\bar{Y}_i = \frac{1}{N}\sum_{j=1}^{N} Y_{ij}, \tag{4}$$

where $N = 7$. The average temperature histories at both the mica/specimen and specimen/insulation interfaces are shown in Fig. 2. The mica/specimen temperature history contains much more information regarding the surface q and thus it is the only one used herein. The estimated standard deviation at *each* time t_i is calculated using

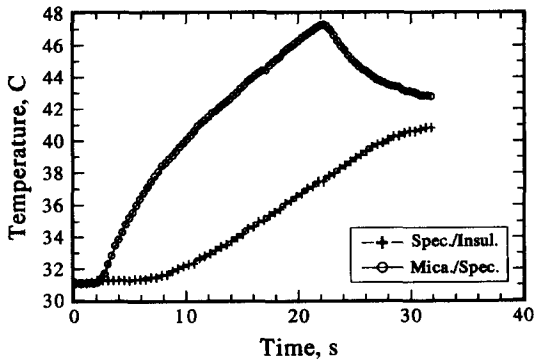

Fig. 2. Sensor-averaged, transient temperatures at the mica/specimen and specimen/insulation interfaces from experiment.

$$\hat{\sigma}_{\bar{Y}_i} = \left[\frac{1}{N(N-1)}\sum_{j=1}^{N}(Y_{ij}-\bar{Y}_i)^2\right]^{1/2} \tag{5}$$

which varies as shown in Fig. 3. It is roughly constant during the heating period (2–22 s) at about 0.115 K and about 0.04 when the heater is off. For simplicity the average of the standard deviations in Fig. 3 is used, which is about 0.083 K, and is shown. This is the value that is to be used in the residual principle for the various regularizing parameters. The estimated heat fluxes are not usually sensitive to this assumption. In the remainder of the paper $\bar{Y}_i$ will be simply written as Y_i.

IHCP ESTIMATION METHODS

There are many methods for solving the IHCP. Those used herein are described briefly. The function specification method is described first. It can be used for linear and nonlinear problems; finite differences, finite elements, or numerical convolution can be used; and various approximations for specified functions are possible. Briefly the method is to minimize with respect to the heat flux q_M the sum of squares function,

$$S_M = \sum_{i=1}^{r}(Y_{M+i-1} - T_{M+i-1})^2 \tag{6}$$

which involves the times $t_M, t_{M+1}, \ldots, t_{M+r-1}$. [Only one temperature sensor is assumed in equation (6).] Hence, 'future' information is used to obtain q_M. Some

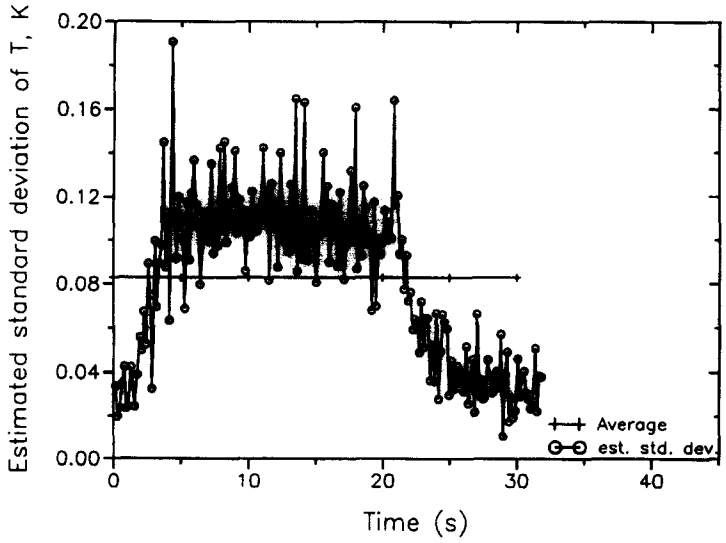

Fig. 3. Standard deviation of average temperature at the mica/specimen interface.

functional form for $q(t)$ for t_{M-1} to t_{M+r-1} is selected, the simplest being

$$q_{M+i-1} = q_M, \quad i = 1, 2, \ldots, r. \tag{7}$$

The calculated temperature T_{M+i-1} is expanded in a Taylor series for q_M,

$$T_{M+i-1} = T_{M+i-1}|_{\hat{q}_{M-1}} + X_{M+i-1,M}(q_M - \hat{q}_{M-1}), \tag{8}$$

where $X_{M+i-1,M}$ is the sensitivity coefficient defined by

$$X_{M+i-1,M} = \frac{\partial T_{M+i-1,M}}{\partial q_M}. \tag{9}$$

The resulting algorithm after minimizing equation (6) with respect to q_M is

$$\hat{q}_M = \hat{q}_{M-1} + \frac{\sum_{i=1}^{r} [Y_{M+i-1} - T_{M+i-1}|_{q_M = \cdots = \hat{q}_{M-1}}] X_{M+i-1,M}}{\sum_{i=1}^{r} X_{M+i-1,M}^2}. \tag{10}$$

Only $\hat{q}_M$ is retained for time t_M, and M is increased by one and the procedure is repeated. In this paper, the r value is selected using the residual principle. The bias caused by the algorithm is also significant [8], but is not considered here.

The iterative regularization method minimizes the whole domain function

$$S = \sum_{i=1}^{I} (Y_i - T_i)^2, \tag{11}$$

where I is the total number of measurements (about 200 in this experiment). The iterative regularization method of Alifanov [1] uses two solutions besides the direct problem [equations (1, 2)]. These solutions are the sensitivity and adjoint problems. Moreover, the conjugate gradient method is used. More details are given in refs. [1, 10]. The stopping parameter is the number of iterations, which is determined by the residual principle. For the same number, I, of measurements as q components, the minimum of S is zero for equation (11), resulting in an ill-posed and unstable method for small time steps. However, if the number of iterations is limited by the residual principle, the method becomes stable, but S is *not* minimized. It is a nonlinear method, even if the differential equations are linear.

Zeroth-order Tikhonov regularization adds a term to S defined by equation (11) to get

$$S = \sum_{i=1}^{I} (Y_i - T_i)^2 + \alpha \sum_{i=1}^{I} q_i^2, \tag{12}$$

where α is the regularization parameter. In this method, S is minimized and it can be done many ways. For many components and whole domain estimation the adjoint-conjugate gradient method is appropriate [1, 10]. In Tikhonov regularization, the minimum of S given by equation (12) is not zero. The parameter α is chosen using the residual principle [1, 13].

In each of the above methods it is necessary to describe the variation of $q(t)$. A simple method is to approximate the heat flux by constant segments,

$$q(t) = q_M, t_{M-1} < t < t_M, \tag{13}$$

where $t_M = M\Delta t, M = 1, 2, \ldots, I$. Another approximation is linear interpolation,

$$q(t) = \hat{q}_{M-1} + (q_M - \hat{q}_{M-1}) \frac{t - t_{M-1}}{\Delta t} \tag{14}$$

for $t_{M-1} < t < t_M$.

For the FSM (and other methods), many tem-

porary specified functions are possible including the constant given by equation (7). For example, there is linear with time,

$$q_{M+i-1} = \hat{q}_{M-1} + (q_M - \hat{q}_{M-1})\tau_i \qquad (15)$$

$$\tau_i = \frac{t_{M+i-1} - t_{M-1}}{\Delta t}, \quad 0 < \tau_i < r. \qquad (16)$$

The r symbol denotes the number of 'future' time steps. A parabolic approximation with a zero value for the first time derivative at $\tau_i = r$ is

$$q_{M+i-1} = \hat{q}_{M-1} + (q_M - \hat{q}_{M-1})\frac{2r\tau_i - \tau_i^2}{2r-1}. \qquad (17)$$

A cubic approximation with zero values for the first and second time derivatives at $\tau_i = r$ is

$$q_{M+i-1} = \hat{q}_{M-1} + (q_M - \hat{q}_{M-1})\frac{3r^2\tau_i - 3r\tau_i^2 + \tau_i^3}{3r^2 - 3r + 1}. \qquad (18)$$

RESULTS

A measure of the difference between the measured and calculated temperature is needed. It should be analogous to the standard deviation of the data, which is known in the present case. An expression for the estimated standard deviation of the measured temperature Y_i is,

$$s_Y = \left[\frac{1}{I-1}\sum_{i=1}^{I}(Y_i - \hat{T}_i)^2\right]^{1/2}, \qquad (19)$$

where $\hat{T}_i$ is the calculated temperature. This expression can be used even if there is no prior estimate of the measurement errors.

A similar equation to equation (19) can be given if the true applied heat flux is known,

$$\hat{\sigma}_{q_{\text{rms}}} = \left[\frac{1}{I-1}\sum_{i=1}^{I}(q_i - \hat{q}_i)^2\right]^{1/2}, \qquad (20)$$

where q is the measured heat flux and $\hat{q}$ is the estimated value using an IHCP algorithm. It is only because the heat flux is *measured* in this problem that equation (20) can be evaluated. Note that there is a difference in the interpretation of equations (19) and (20). In equation (19), Y_i is assumed to contain measurement errors, while in equation (20) q_i is assumed to be nearly errorless; furthermore, $\hat{\sigma}_{q_{\text{rms}}}$ contains errors from both errors in Y and bias in the algorithm [8]. Because the interpretations of equations (19) and (20) are different, different symbols are chosen.

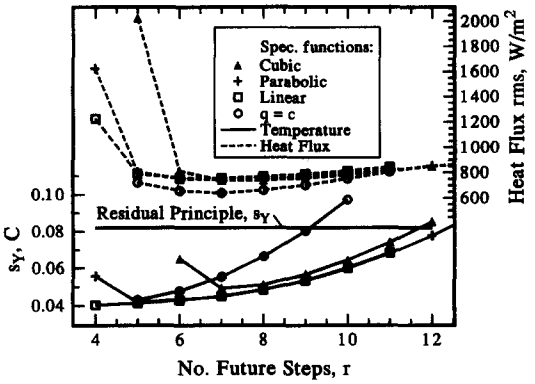

Fig. 4. Estimated temperature standard deviation and heat flux r.m.s. using the function specification method vs the number of future time steps.

FUNCTION SPECIFICATION RESULTS

Figure 4 shows values for s_Y and $\hat{\sigma}_{q_{\text{rms}}}$ (solid and dashed lines, respectively) for the FSM as a function of the number of future time steps r. Four cases are shown: q approximated as constant, linear, parabolic and cubic functions. One way of stating the residual principle is that the regularizing parameter, r, is found by making the estimated standard deviation of the data about equal to the expected s_Y. For the $q = C$ approximation, the value of r equal to 9 or 10 is obtained from Fig. 4 at the expected value of $s_Y = 0.083$. For the other cases, a value of about $r = 12$ or 13 is appropriate; the value of $r = 13$ is selected. These are large r values, indicating that the data shown by Fig. 2 poses a challenge for the methods which try to follow detailed changes in q.

Also observe the $\hat{\sigma}_{q_{\text{rms}}}$ curves (the dashed lines) in Fig. 4. The minimum value is for the $q = C$ approximation with the others slightly larger. For all cases the $\hat{\sigma}_{q_{\text{rms}}}$ values shown in Fig. 4 are less than 10% of the maximum $q(t)$, which is about 7800 W m^{-2}. See the lowest dashed curve in Fig. 5 and the lower right axis. An important point is that the $\hat{\sigma}_{q_{\text{rms}}}$ values are insensitive to r. This is a good feature of the FSM. For a given case, the minimum $\hat{\sigma}_{q_{\text{rms}}}$ does not precisely correspond to the r value given by the residual principle. However, these curves vary so gradually that the choices of r given by the residual principle are quite acceptable.

The results for the estimated heat flux using the Fig. 2 data are shown in Fig. 5. Several curves are shown by displacing one above the other; if the curves were plotted on the same axes, the values overlap and become indistinguishable.

There are several obvious features of the results. First, there is smoothing of the abrupt increases and decreases. Second, the results are not identical, but are remarkably close. The cubic curve for $r = 13$ is not markedly better than the $q = C$ curve for $r = 7$. The human eye favors the cubic results in Fig. 5, but the $\hat{\sigma}_{q_{\text{rms}}}$ is smaller for the $q = C$ solution. The $\hat{\sigma}_{q_{\text{rms}}}$ is

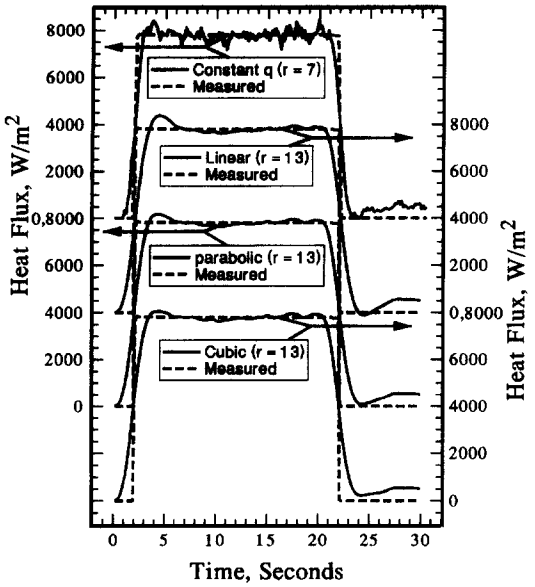

Fig. 5. Estimated heat flux values for the function specification method for constant q basis functions (with $r = 7$, left axis), q linear ($r = 13$, right axis), q parabolic ($r = 13$, left axis) and q cubic ($r = 13$, right axis).

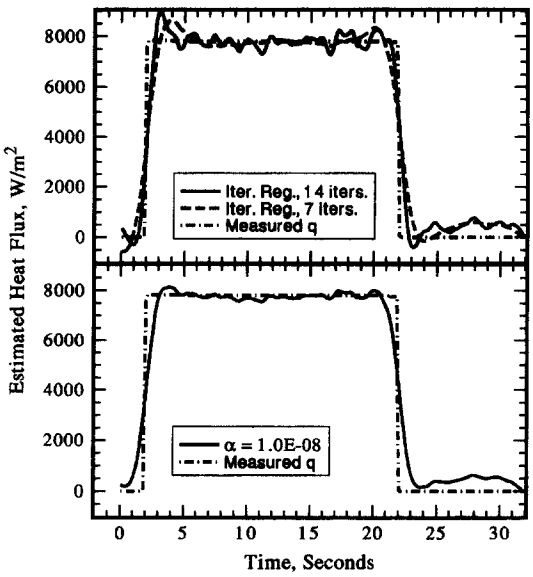

Fig. 7. Estimated heat flux values for the iterative regularization method (upper figure 7 and 14 iterations) and Tikhonov regularization (lower figure for $\alpha = 1.0 \times 10^{-8}$).

greatly affected by the treatment of the values near the abrupt changes (near 2 and 22 s).

Next consider the results obtained by using two whole domain methods. The s_Y and $\hat{\sigma}_{q_{rms}}$ values (lower and upper sets of curves, respectively) are shown in Fig. 6 for the four cases: iterative regularization and Tikhonov regularization with $\alpha = 10^{-9}$, 5.0×10^{-9} and 10^{-8} K^2 m^4 W^{-2}. From the residual principle, about seven iterations are needed for the iterative regularization method and for Tikhonov regularization α should be about 10^{-8} K^2 m^4 W^{-2} (from Fig. 6 to have $s_Y \approx 0.083$ C). Notice that the $\hat{\sigma}_{q_{rms}}$ values are about the same values for the iterative regularization method with seven iterations as obtained using the FSM, that is about 700 W m^{-2} compared with the maximum value of 7800 W m^{-2}. The $\hat{\sigma}_{q_{rms}}$ decreases with the number of iterations until 14 and then starts to increase. The optimal α for Tikhonov regularization (10^{-8}) gives about the same value of $\hat{\sigma}_{q_{rms}}$ (about 700 W m^{-2}). Tikhonov regularization takes considerably more iterations than iterative regularization, even though both use the same direct, sensitivity and adjoint-equations, coupled with the conjugate gradient method. For this case of about 200 measurements, the Tikhonov regularization method converges in less than 28 iterations.

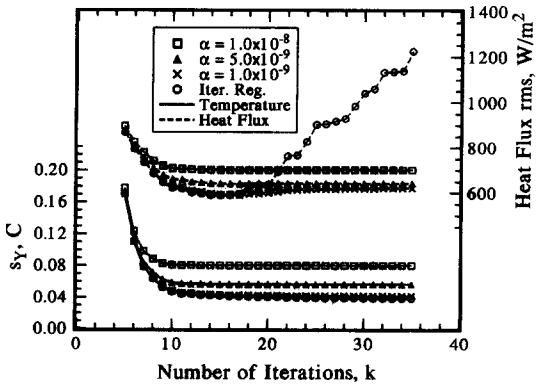

Fig. 6. Estimated temperature standard deviation and heat flux r.m.s. using the iterative and Tikhonov regularization methods vs the number of iterations.

The iterative regularization is investigated for both the $q = C$ and linear approximations (using the whole domain approach). The results are indistinguishable for the same number of iterations. Figure 7 shows the estimated heat fluxes for both seven (the residual principle value) and 14 (the minimum $\hat{\sigma}_{q_{rms}}$ value) iterations. The seven iteration results are appreciably better to the eye than the 14 iteration case. The reason that the $\hat{\sigma}_{q_{rms}}$ values in Fig. 6 are opposite is the difference in values near the step increase/decrease, which is very difficult for the human eye to assess.

Two other features of the iterative regularization method are significant. Note that just before heating starts and just after it stops, some slight negative heat fluxes are estimated, unlike the FSM. The second feature is that the final estimated q (about 32 s) is zero. This is because the beginning estimate for all the qs is zero and there is a lag in the temperature response, so that no information regarding the heating has been received in the T regarding q at the final time. The FSM does not attempt to give a q value at the final measured time, instead it stops $r-1$ steps before the end.

Figure 7 also shows the Tikhonov regularization results for 28 iterations (convergence) for $\alpha = 10^{-8}$. The results are similar to those for the iterative regularization method for seven iterations, except the

behavior is better in Fig. 7 both before and after the steps, since there are no negative heat flux values before heating starts.

If one compares the results from the different methods given above, it is amazing how close the agreement is, even though quite different methods are used. Based only on the minimum value of $\hat{\sigma}_{q_{rms}}$ in Fig. 6, the iterative regularization with about 14 iterations or Tikhonov regularization with 10^{-9} K^2-m^2 W^{-2} are equivalent and have $\hat{\sigma}_{q_{rms}} \approx 600$ W m^{-2}. Using the same criterion, the best result for FSM in Fig. 4 has the minimum value of 620 W m^{-2}, which is for the $q = C$ profile. These results correspond to values of s_Y somewhat less than that indicated by the residual principle, as used herein. For example, instead of 0.083°C, the values for minimum $\hat{\sigma}_{q_{rms}}$ are 0.055 and 0.043°C, for Figs. 4 and 6, respectively.

INVERSE HEAT CONDUCTION USING GREEN'S FUNCTIONS

The Green's function solution method becomes an integral equation when it is applied to linear inverse heat conduction problems. The function specification method reduces this integral equation to a set of simultaneous linear equations. For the sake of brevity, the following presentation is for a one-dimensional temperature field, although the procedure is equally applicable to multidimensional solutions. The alternative Green's function solution method [16, equation (3.66)] is

$$T(y,t) = T^*(y,t) + \int_0^L G(y,t|y',0)[T(y',0) - T^*(y',0)]\,dy' + \frac{\alpha}{k}\int_0^t \int_0^L G(y,t|y',\tau) \times \left[k\frac{\partial^2 T^*(y',\tau)}{\partial y'^2} - \rho c \frac{\partial T^*(y',\tau)}{\partial \tau}\right] dy'\,d\tau, \quad (21)$$

where L is the thickness of the solid and $T^*(y,t)$ is a differentiable function that satisfies the same homogeneous boundary conditions as $T^*(y,t)$. If $q_1(t)$ is the heat flux at $y = 0$ and $q_2(t)$ is the heat flux at $y = L$, then, a typical function for $T^*(y,t)$ is

$$T^*(y,t) = \frac{y^2}{2Lk}[q_1(t) - q_2(t)] - \frac{y}{k}q_1(t). \quad (22)$$

In this approximation, the functions $q_1(t)$ and $q_2(t)$ are

$$q_i(t) = a_{i0} + a_{i1}t + a_{i2}t^2 + \cdots; \quad i = 1,2. \quad (23)$$

The substitution of $T^*(y,t)$ in equation (21) yields a linear relation for every measured internal temperature. Since there are more measurements than unknown parameters, least squares is used.

The same set of data employed earlier was used to predict surface heat flux for a carbon–carbon sample.

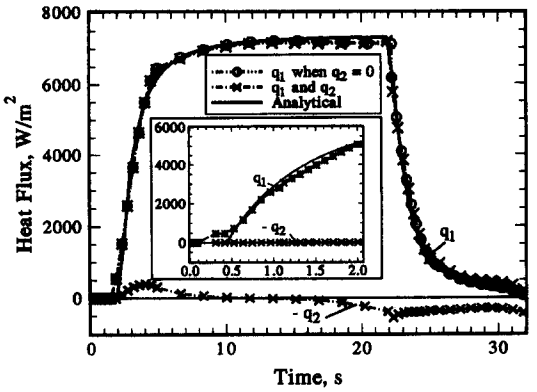

Fig. 8. Estimated heat flux values at the mica–specimen interface using Green's functions and polynomial approximations over extended time regions.

It is assumed that the 7800 W m^{-2} heat flux starts at $t = 1.9$ s at the *heater site* and the power is ended at 21.9 s. The surface heat flux from *mica to carbon–carbon* is analytically computed and the results are plotted in Fig. 8 as a solid line. Notice the damped and lagged response at the mica/C–C interface compared to the heater input. The inverse conduction Green's function procedure is then used to predict the surface heat flux at this interface. The reason that this heat flux at the interface was estimated rather than at the heater/mica interface (as above) is that the use of a small number of constant-in-time functions (for carefully-selected time regions) matches the input heat flux almost precisely using Green's functions (and other solution methods). However, at the mica/specimen interface, the heat flux cannot be as simply described, but q can be approximated by polynomials.

Two cases are considered: one estimating q_1 with $q_2 = 0$ and the other case estimating both q_1 and q_2. Measured temperature data at two thermocouple sites (mica/specimen and specimen/insulation interfaces) were used.

Figure 8 shows the calculated heat flux q_1 denoted by circles for the case assuming $q_2 = 0$. Based on examination of the temperature data, the duration of the test was divided into five time domains, 0–1.5, 1.5–4.9, 4.9–21.9, 21.9–25 and $t > 25$. The boundary between two adjacent time domains was chosen where the change in dT/dt is large. Future time at the end of each time domain was added to improve the accuracy of computations. A smaller region of future time was added when the change in dT/dt are abrupt, e.g. 0.16 s after the first time and the third time domains. This is because a large number of future steps can adversely influence the results when abrupt changes occur. The open circle data in Fig. 8 are the results of the computations and they agree very well with the direct analytical solution.

The next step in this computation method is to simultaneously predict q_1 and q_2 using the same set of experimental data. The results are also plotted in Fig. 8 and can be compared with the other results. Figure

8 shows that the effect of q_2 on q_1 is small. The two sets of q_1 results are nearly identical for $t < 26$ s. Also, the calculated values of q_2 are small until $t = 15$ s. To study the effect of the initial rise in temperature, a second set of experimental data was used. The data were measured at 0.01 s time steps for a total period of 2.19 s. The results are shown in the inset of Fig. 8. The value of q_2 is negligibly small.

It is clear that the results using the Green's function with extended regions worked very well in this case. In the various methods described first, the surface heat flux is estimated at every time step. This has the advantage that it can be used in cases when the heat flux has rapid changes, such as in quenching, as well as slowly varying changes; the time periods for these conditions do not have to be specified. A disadvantage of the first methods is that the results show some fluctuations caused by the measurement errors and the ill-posed nature of the problem. When the heat fluxes do not exhibit rapid variations (or the moments of rapid changes can be inferred), it is possible to produce smoothly varying heat fluxes by dividing the domain into a few regions. In such cases and for linear problems, the method of solution of the heat conduction equation, whether using an analytical method (such as Green's functions) or a numerical method (such as finite differences), will produce almost identical results. For convenience in presentation, the smoothing procedure by using low degree polynomials of different regions is described using the Green's functions; however, each of the methods given above will give almost identical results to those shown in Fig. 8 if the same polynomial approximations are used.

COMPARISON OF COMPUTER TIME

Two other aspects of comparison of the FSM and the regularization methods are mentioned. One is the simplicity of derivation. The FSM is simpler to derive because special sensitivity and adjoint equations do not have to be derived. Furthermore, for the present one-dimensional example, the FSM estimates are about as accurate as those produced by the iterative and Tikhonov (zeroth-order) regularization. In other cases it has been found that the FSM method is not quite as accurate as the regularization methods [8].

The second aspect relates to the computation time. The calculations were performed using about 200 time steps. In order to avoid questions regarding space discretization and also calculation of time steps, the computer times were obtained using numerical approximations of Duhamel's integral. Some finite difference calculations were independently performed both to verify the results and to obtain the solution for a unit step heat flux, which is needed in Duhamel's integral. In each of the above cases there is no temperature-variation of the thermal properties, hence no iterations are needed. A 486 IBM compatible 50 Mz computer was used with Microsoft FORTRAN. The FSM for $r = 7$ and 13 took 1.42 and 1.54 s, respectively. Hence, there is little difference in computer time between the $r = 7$ case the case of almost twice as large value r of 13. That behavior is not replicated for iterative and Tikhonov regularization (both depend mainly on the number of iterations). For seven iterations and computation time is 2.53 s and for 28 iterations the time is about four times as large (9.61 s). The FSM is more computationally efficient than the whole domain methods considered herein for the example considered.

Other cases may yield different results; however, the analytical study of ref. [10] tends to confirm these results which use experimental data.

SUMMARY AND CONCLUSIONS

Several methods are compared for the solution of the inverse heat conduction problem of estimating the transient surface heat flux from interior temperature histories. This paper is unique in using actual temperature measurements and a known electrical heat input. The methods include the function specification method, iterative regularization, Tikhonov regularization and Green's functions with the heat flux approximated by polynomials over a few time periods.

The function specification method gave accurate results and is computationally efficient. The results using the iterative regularization method are excellent. Zeroth-order Tikhonov regularization gives comparable results. However, the computation time is a factor of 2–4 as large for the Tikhonov vs iterative regularization.

An important observation is that the three methods just mentioned above give excellent, but very similar, results. However, the function specification method is conceptually simpler and can be extended more readily to other parabolic problems.

The Green's function method with extended time regions approximated by polynomials gave excellent results. The concept of using polynomials over extended time regions can be used with the other methods and almost identical results are obtained.

Acknowledgements—This research was partially supported by the Research Excellence Fund of the State of Michigan through the Composite Materials and Structures Center at Michigan State University and Sandia National Laboratories, Albuquerque, NM under U.S. Air Force Contract FY1456-91-N0058.

REFERENCES

1. O. M. Alifanov, *Inverse Heat Transfer Problems*. Springer, New York (1994).
2. N. V. Shumakov, A method for the experimental study of the process of heating a solid body. *Sov. Phys. Tech. Phys.* (Translated by American Institute of Physics) **2**, 771–781 (1957).
3. G. Stolz, Jr, Numerical solutions to an inverse problem of heat conduction for simple shapes, *J. Heat Transfer* **82**, 20–26 (1960).
4. J. V. Beck, Calculation of surface heat flux from an

internal temperature history, ASME Paper 62-HT-46 (1962).
5. J. Beck, Nonlinear estimation applied to the nonlinear inverse heat conduction problem, *Int. J. Heat Mass Transfer* **13,** 703–715 (1970).
6. J. V. Beck, Criteria for comparison of methods of solution of the inverse heat conduction problem, *Nucl. Engng Des.* **53,** 11–22 (1979).
7. J. V. Beck, B. Litkouhi and C. R. St. Clair, Jr, Efficient sequential solution of the nonlinear inverse heat conduction problem, *Numer. Heat Transfer* **5,** 275–286 (1982).
8. J. V. Beck, B. Blackwell and C. R. St. Clair, Jr, *Inverse Heat Conduction: Ill-posed Problems*. Wiley, New York (1985).
9. A. M. Osman and J. V. Beck, Nonlinear inverse problem for the estimation of time-and-space-dependent heat-transfer coefficients, *J. Thermophys. Heat Transfer* **3,** 146–152 (1989).
10. J. V. Beck, Comparison of the iterative regularization and function specification algorithms for the inverse heat conduction problem. In *Inverse Problems in Engineering: Theory and Practice* (Edited by N. Zabaras, K. Woodbury and M. Raynaud) pp. 23–30. ASME, New York (1993).
11. D. A. Murio, *The Mollification Method and the Numerical Solution of Ill-Posed Problems*. Wiley–Interscience, New York (1993).
12. A. N. Tikhonov and V. Y. Arsenin, *Solutions of Ill-Posed Problems*. V. H. Winston, Washington, DC (1977).
13. O. M. Alifanov, E. A. Artyukhin and S. V. Rumyantsev, *Extreme Methods for Solving Ill-Posed Problems with Applications to Inverse Heat Transfer*. Begell House, New York (1995).
14. J. V. Beck and K. J. Arnold, *Parameter Estimation in Engineering and Science*. Wiley, New York (1977).
15. K. Dowding, J. Beck, A. Ulbrich, B. Blackwell and J. Hayes, Estimation of thermal properties and surface heat flux in a carbon–carbon composite material, *J. Thermophys. Heat Transfer* **9,** 345–351 (1995).
16. J. V. Beck, K. Cole, A. Haji-Sheikh and B. Litkouhi, *Heat Conduction Using Green's Functions*. Hemisphere, Washington, DC (1992).